Centrifuge Shaking Table Test on Pile Foundation Combined with Soil-cement Mixing Walls as Permanent Pile

Koji WATANABE, Makoto ARAKAWA & Minoru MIZUMOTO
Technical Research Institute of Obayashi Corporation, Kiyose, Tokyo, Japan

ABSTRACT
Soil-cement mixing walls are often used for temporary structures as earth retaining walls when the ground is excavated. However, when soil-cement mixing walls are used as permanent piles, they are expected to support foundation structures. A centrifuge shaking table experiment was conducted on models of pile foundation structures to examine the effect of the presence of soil-cement mixing walls installed at the external peripherals on the responses of piles and structures, to understand the characteristics of foundation structures that use soil-cement mixing walls as permanent piles during earthquakes. This report describes the findings from the centrifuge shaking table experiment.
A shear box was used for this experiment with a centrifuge acceleration of 50 G and a model scale of 1/50. The structure models used consisted of Model N that simulated the pile foundation and Model S that used soil cement column walls arranged on the periphery of the pile foundation. A sinusoidal wave was used for the input, and four cases of shakings that varied in shaking frequencies and acceleration amplitudes were performed. Moreover, an earthquake wave was also used for the input, and shaking that varied in acceleration amplitudes was also performed.
The following findings from the centrifuge shaking table experiment were described as follows.
1) There are cases where the shaking response increases for a building with a foundation structure utilizing soil-cement mixing walls as permanent piles. However, this response increase is dependent on the shaking characteristics of the input waves.
2) The bending moment and shearing force are confirmed to be reduced by the soil-cement mixing walls. Finally, appropriately evaluating the impact of the frictional force acting on the soil-cement mixing walls is considered important in order to quantitatively evaluate the amount of reduction in the pile stress.

1 INTRODUCTION

A soil-cement continuous column wall (hereafter, soil-cement mixing wall) is constructed by inserting core material, which acts as a stress transfer material, into soil-cement formed by injection of cement milk into the center of the soil, and then churning and mixing the ground foundation. The soil-cement continuous column wall has previously been used as an earth retaining wall during excavations, and was treated as a temporary structure. At present, a method has not been established for evaluating its assumed seismic behavior when bearing a building body load or something similar. In recent years, rationalization of the foundation structure, reduction of the environmental burden, and other needs have been rising, and as shown in Figure 1, studies have been proceeding into the use of soil-cement continuous column walls as permanent piles (Watanabe et al. 2013, Watanabe et al. 2014, Watanabe et al. 2015). In addition, with the previously temporary soil-cement mixing wall now being used as a permanent pile, it can be expected that eliminating the need for new work and reduce construction expenses.

There have been some studies on vertical bearing capacity where earth retaining walls are used as permanent piles, and these studies focused on full-scale load or construction tests. Kaneko (2004) is constructing high-strength soil-cement mixing walls, developing methods for their use as permanent piles, and evaluating their bearing capacities. Taya et al. (2009) are improving construction control methods and construction equipment, constructing high-strength soil-cement walls, and evaluating their bearing capacities. Both of these walls

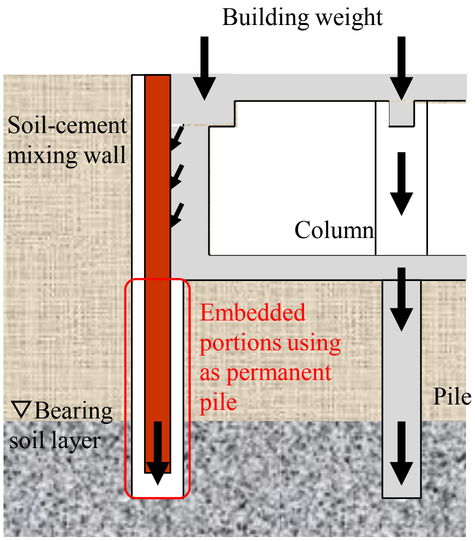

Figure 1. Concept of utilization for permanent pile of soil-cement mixing wall

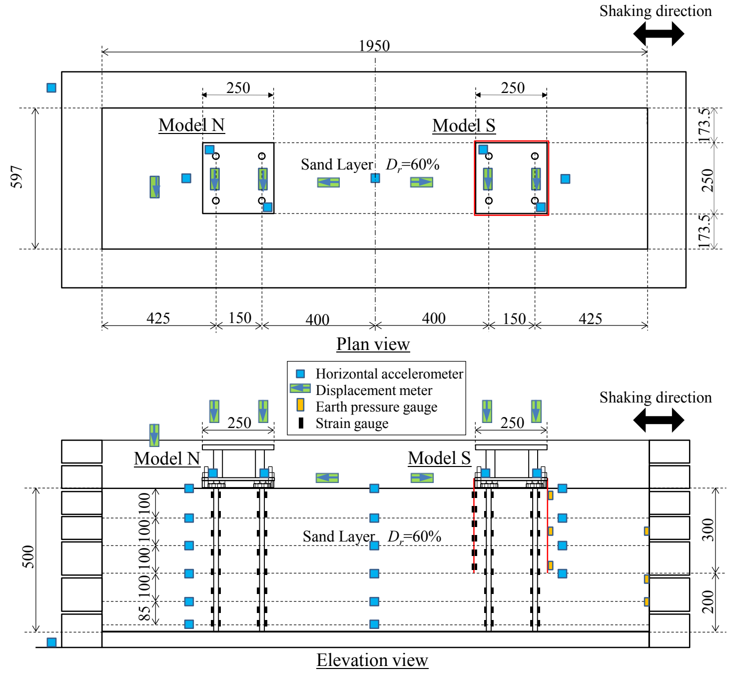

Figure 2. Schematic view of centrifuge shaking table test (Unit: mm)

Table 1. Model specifications

	Model scale (1/50)	Prototype scale
Planner dimension of building	250×250mm	12.5×12.5m
Upper part mass	8.58kg	1070t
Foundation mass	7.46kg	933t
Natural frequency of building	556Hz	11.1Hz
Length of pile	500mm	25.0m
Length of soil-cement mixing wall	275mm	13.75m

Table 2. Input wave conditions

Case	Inlput wave	Frequency (Hz)	Maximum input acceleration (m/s^2)
Case L1	Sinusoidal wave	1.2	0.6
Case L2			3.0
Case H1		2.4	0.8
Case H2			3.0
Case R1	Rinkai wave	-	0.5
Case R2			3.3

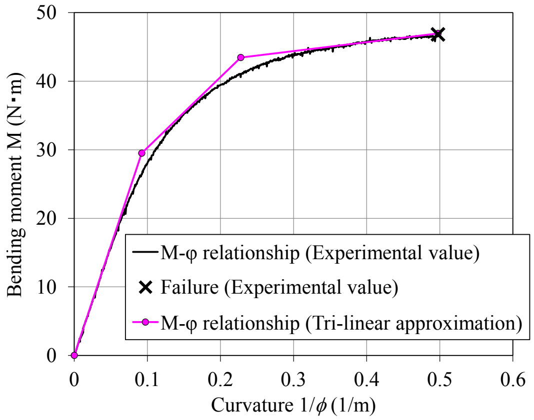

Figure 4. *M*–*φ* relationship based on pile bending test (Model scale)

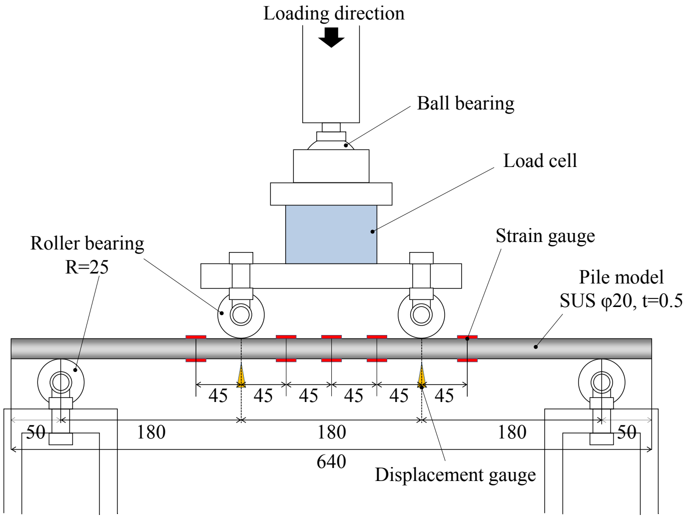

Figure 3. Schematic view of pile bending test (Unit: mm)

differ from the soil-cement walls in general use, in that they assume construction of high-strength soil-cement mixing walls.

Use of soil–cement mixing walls as permanent piles is promising from a foundation structure rationalization standpoint, but the horizontal seismic behavior needs to be evaluated, as many aspects of the seismic behavior of foundation structures that include the soil–cement mixing walls remain unknown. Accordingly, in order to determine the effect of presence/absence of soil–cement mixing walls on the response of foundation structures, centrifuge shaking table tests were conducted on the foundation structures, wherein the soil–cement mixing walls were used as permanent piles. This study presents the method and results of the centrifuge shaking table tests.

2 CENTRIFUGE SHAKING TABLE TESTS

Figure 2 shows the schematic view of centrifuge shaking table test. A shear soil container was used in the shaking table test, and the model ground was created using air-pluviation method such that the relative density of the D_r was 60%. Silica sand No. 7 (Specific gravity of soil, G_s=2.645) was used in preparing the model ground. For the foundation, the pile foundation of the building was simulated using Model N, whereas Model S simulated the soil–cement mixing wall around the area where the pile foundation perimeter was placed. Table 1 lists the model specifications. The pile model was constructed using stainless steel of diameter 20mm and thickness 0.5mm, and the soil–cement mixing wall model was constructed using an aluminum sheet of thickness 1.5mm. As the model scale ratio was 1:50, a centrifuge acceleration of 50G was used in the shaking table tests. Table 2 lists the input wave conditions for each test cases. In cases L1,

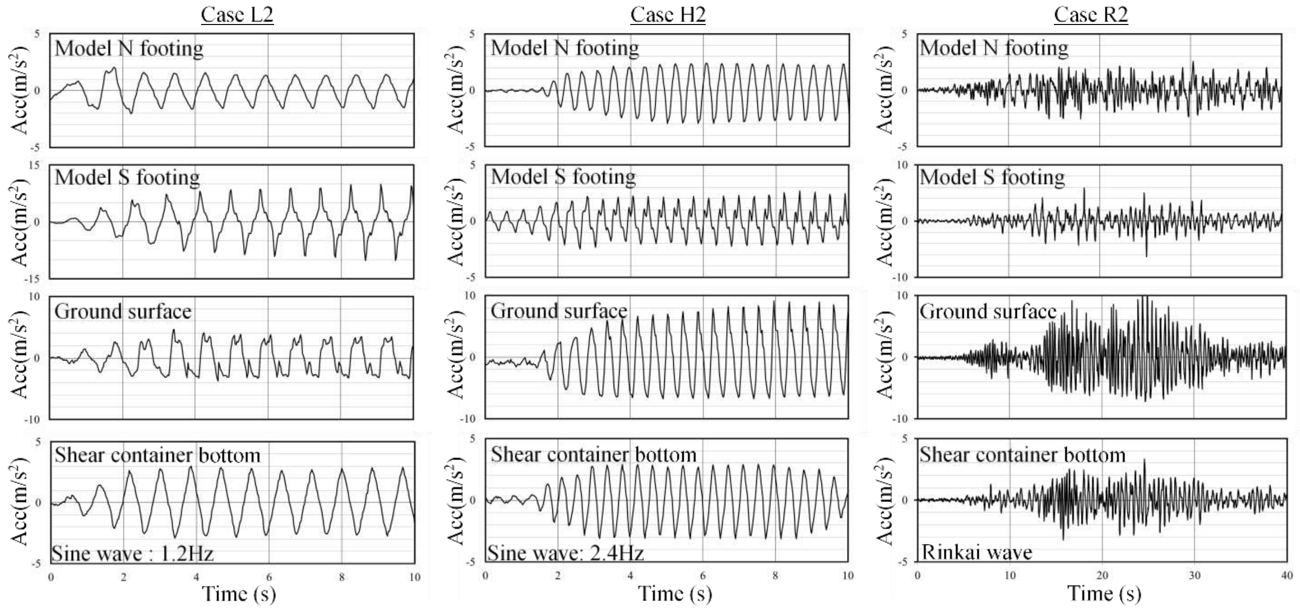

Figure 5. Time history curves of response acceleration

L2, H1, and H2, the frequency and amplitude of acceleration were varied using sine wave as input to generate stepwise shaking. However, in cases R1 and R2, the frequency and amplitude of acceleration were varied using the Rinkai wave (i.e. artificial earthquake wave) as input to generate the shaking. The parameters measured were acceleration at various depths of the model ground and at the foundation footing, displacement of the model structure and at ground level, the strains of the pile model and the soil–cement mixing wall model, and the earth pressure on the soil–cement mixing wall model. It must be noted that the strain at the soil–cement mixing wall model and the earth pressure acting on the soil-cement mixing wall model were measured orthogonally (out-of-plane wall direction) relative to the direction of acceleration.

The test results suggest that the relationship between the bending moment and the curvature of the pile model (*M*–*φ* relationship) is necessary to analyze the stress acting on the model pile in the centrifuge shaking table tests. Accordingly, the *M*–*φ* relationship for the model pile was evaluated through experiments, wherein four-point bending tests were conducted on the pile models, similar to those used in the centrifuge shaking table tests. Figure 3 shows the schematic of the bending tests. In the tests, the support and load points were in contact with the test specimen via free rotating rollers. The parameters measured for the test specimen were the bending strains at the upper end compression side and the lower end tension side, and the displacement at the loading point. Figure 4 shows the relationship between the bending moment, as calculated from the test load, and the curvature, as calculated from the bending strain at the center of the test specimen. As observed from Figure 4, during initial loading, the relationship between the bending moment and the curvature is nearly linear, but as the curvature increases, the gradient of curve gradually decreases. The maximum bending moment was 47 Nm. Based on the aforementioned test results, Figure 4 shows the tri-linear approximation of the *M*–*φ* relationship. It is understood that the tri-linear approximation of the *M*–*φ* relationship obtained from the bending tests enabled accurate modeling. Accordingly, the *M*–*φ* relationship approximation, as depicted in Figure 4, was used in calculating the bending moment acting on the model pile in the centrifuge shaking table tests.

3 RESULTS OF CENTRIFUGE SHAKING TABLE TESTS

This Chapter describes the results of centrifuge shaking table tests. The contents are shown as follows;

3.1 Response acceleration of structure
3.2 Bending Moment Acting on Pile and Soil-cement Wall
3.3 Shear Force Acting on Pile and Soil-cement Wall

3.1 Response Acceleration of Structure

Figure 5 shows the acceleration responses of the bottom of the shear container, ground surface, and the footing of the structures for cases L2, H2, and R2. As similar observations of the acceleration response were made for cases L1, H1, and R1, Figure 5 shows only the cases where the input wave level for excitation was high. The acceleration amplitudes at the bottom of the shear container for cases L2, H2, and R2 were 3.0 m/s^2, 3.0 m/s^2, and 3.3 m/s^2, respectively. In contrast, the acceleration amplitudes at the ground surface for cases L2, H2, and R2 were 4.0 m/s^2, 8.0 m/s^2, and 10 m/s^2, respectively. The results suggest that the ground response was significantly amplified in cases H2 and R2 compared to that of case L2.

Moreover, in case H2, the acceleration responses at the footings were 5.0 m/s^2 and 4.0 m/s^2 for Model N and

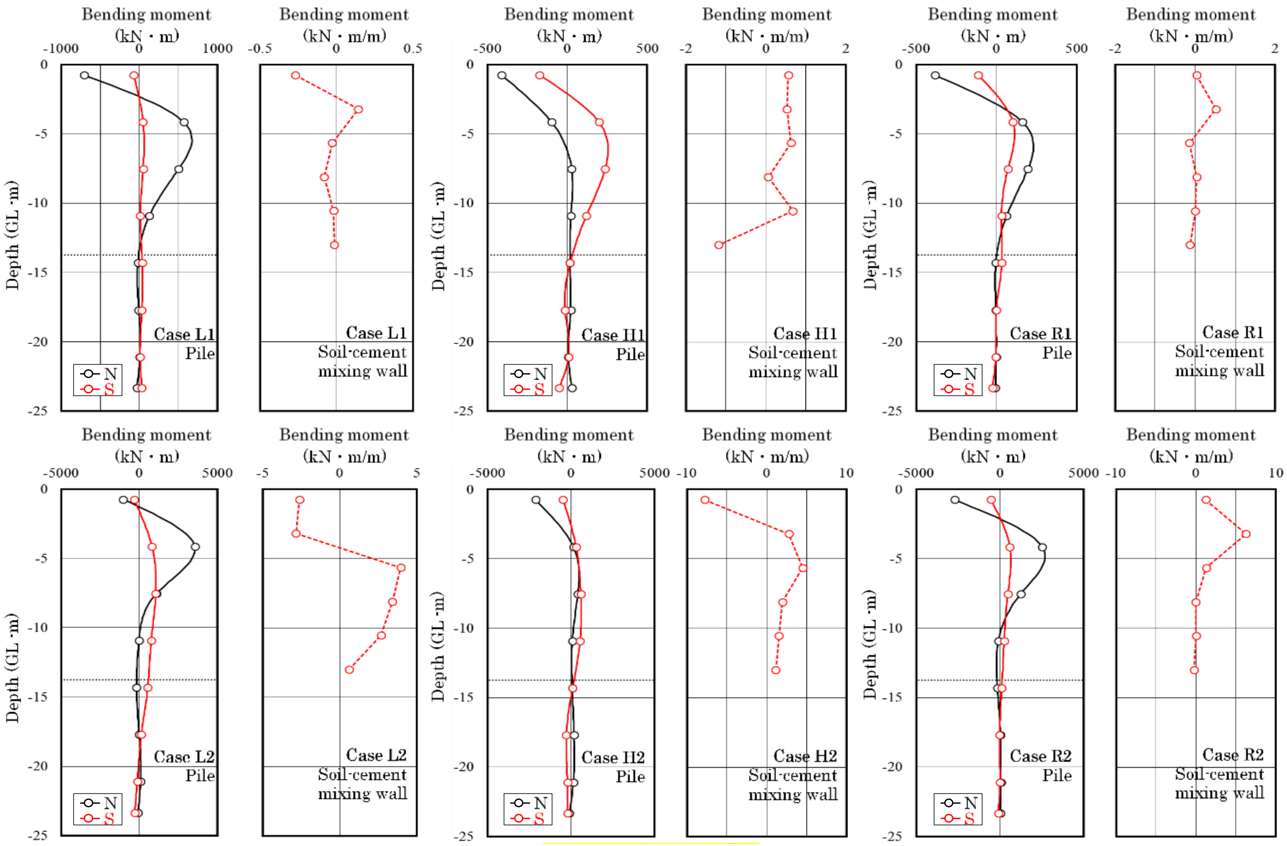

Figure 6. Distribution of bending moment

Model S, respectively, implying that the generated acceleration response was significantly lower for cases with the soil–cement mixing walls. In contrast, in case L2, the acceleration responses at the footings were 1.5 m/s^2 and 9.0 m/s^2 for Model N and Model S, respectively, implying that the generated acceleration response was significantly higher for cases with the soil–cement mixing walls. In the case of R2, higher response acceleration was generated with the soil–cement mixing walls. This may be likely due to the changes in the natural frequency of the ground/foundation structure because of the placement of the soil–cement mixing walls. Here, the natural frequency are 3.76sec and 0.29sec for Model N and Model S, respectively. The observations suggest that it is crucial to evaluate the natural frequency of the ground/foundation structure that includes the soil–cement mixing walls, in order to evaluate the seismic acceleration response of the structures where the soil–cement mixing walls are used as a permanent pile (Kaneko and Isemoto, 1998).

3.2 Bending Moment Acting on Pile and Soil-cement Wall

Figure 6 shows the distribution of the bending moment where the bending moment acting on the pile is highest and the bending moment distribution of the soil–cement mixing walls at the same instant. The bending moment on the pile was calculated based on the measured bending strain and the *M*–*φ* relationship shown in Figure 4. The results correspond to one of the representative pile selected from the four piles used in the tests. For the soil–cement mixing walls, the bending moment was calculated from the measured bending strain and the bending stiffness of the material, effectively representing the out-of-plane bending moment per unit of depth of the wall.

As observed in Figure 6, in all cases, the maximum bending moment generated on the Model S pile was lower compared that of Model N. Moreover, in cases L1, H2, R1, and R2, wherein significant reduction in bending moment at the pile head was observed, the soil‑cement mixing walls likely contributed to the reduction in the bending moment on the pile as is evident from the general correlation between the bending moment distributions on the pile and the soil–cement mixing walls. In contrast, in cases H1 and L2, the bending moment acting on the soil–cement mixing walls near the extremities and the top does not correspond well with the bending moment distribution of the pile. A contributing factor may be the following: due to the earth pressure and the friction acting on the soil–cement mixing walls, the bending stress between the wall surface orthogonal to the direction of excitation (out-of-plane wall direction) and the wall surface parallel to the direction of excitation (in-plane wall direction) likely have changed at certain depths.

3.3 Shear Force Acting on Pile and Soil-cement Wall

Figure 7~Figure 9 show the shear force distribution at the time of highest shear force generated on the pile. The

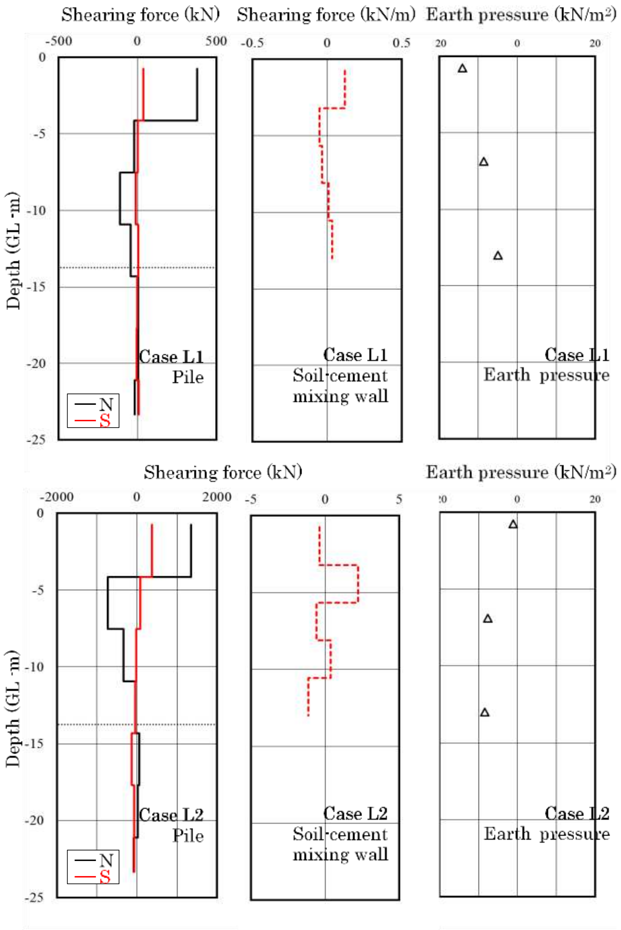

Figure 7. Distribution of shear force and earth pressure (Case L1 and L2)

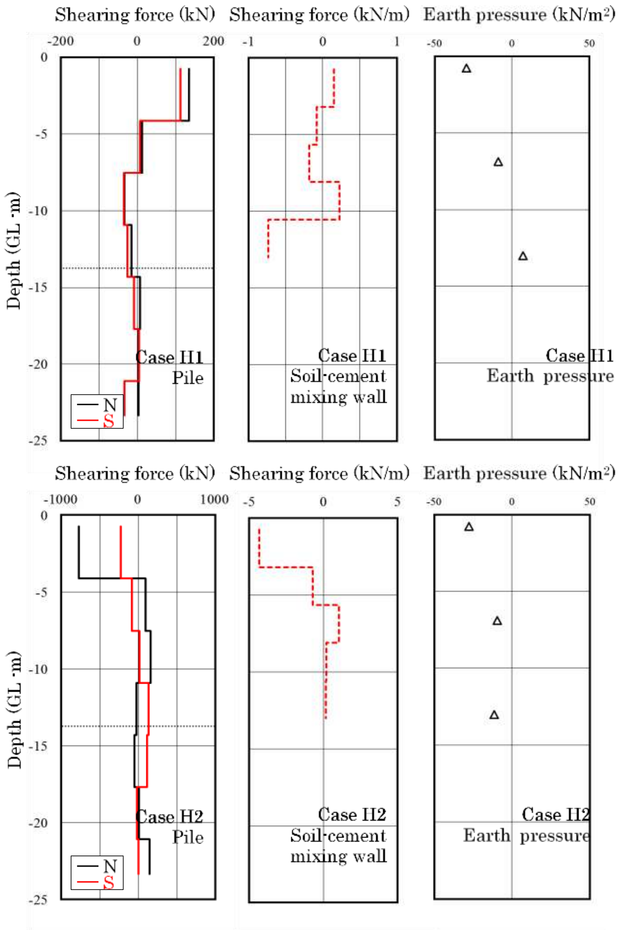

Figure 8. Distribution of shear force and earth pressure (Case H1 and H2)

figures also show the shear force distribution on the soil–cement mixing walls and the earth pressure acting on the walls at the same instant. The shear force was calculated by dividing the bending moment shown in Figure 6 by the distance between the measurement points. Similar to Figure 6, for the piles, the results of only one of the four are shown, and for the soil–cement mixing walls, the out-of-plane wall shear force per unit of depth is shown. Moreover, the earth pressure represents the out-of-plane wall measurement on the soil–cement mixing wall, and shows only the dynamic portion after subtracting the initial earth pressure prior to the excitation. The negative earth pressure represents the passive side and the positive earth pressure represents the active side.

The results shown in Figure 7~ Figure 9 suggest that the maximum shear force on the Model S pile is lower than that of Model N. The results also show that the highest shear force is generated near the pile head in all the piles. In cases L1, H2, and R1, there is an overall agreement between the shearing force distribution on the pile and the soil–cement mixing wall, and the earth pressure becomes highest near the pile head where maximum shear force is generated. It is concluded that the out-of-plane passive resistance of the wall most likely contributes to the reduction in the shear force of the pile. In case of H2, as the shear force per unit width acting on the soil–cement mixing wall in the out-of-plane wall was 4.3kN/m, the overall shear force generated near the top of the out-of-plane wall was estimated to be approximately 110kN. Under such condition, the reduction in the shear force at the head of the pile was 540kN for each pile. Accordingly, the results suggest that compared to the out-of-plane wall passive resistance, the in-plane wall frictional resistance likely contributed more to the reduction in the shearing force at the pile head.

In contrast, in cases L2 and R2, although the earth pressure near the pile head was low, considerable reduction in the shear force at the pile head was observed. It is concluded that the in-plane frictional resistance of the wall contributed more to the reduction in the shear force acting on the pile in these cases.

Based on the aforementioned results, it has been confirmed that although the distribution of the in-plane and out-of-plane wall stresses generated on the soil–cement mixing wall is affected by the earth pressure and the friction, the soil–cement mixing wall contributes to the reduction in the maximum bending moment and the maximum shear force generated on the pile.

Figure 10 shows the variation in the bending strain acting on the pile with respect to time using the Rinkai wave as input and increasing the maximum input acceleration for excitations to 4.4 m/s^2 and 6.0 m/s^2. The

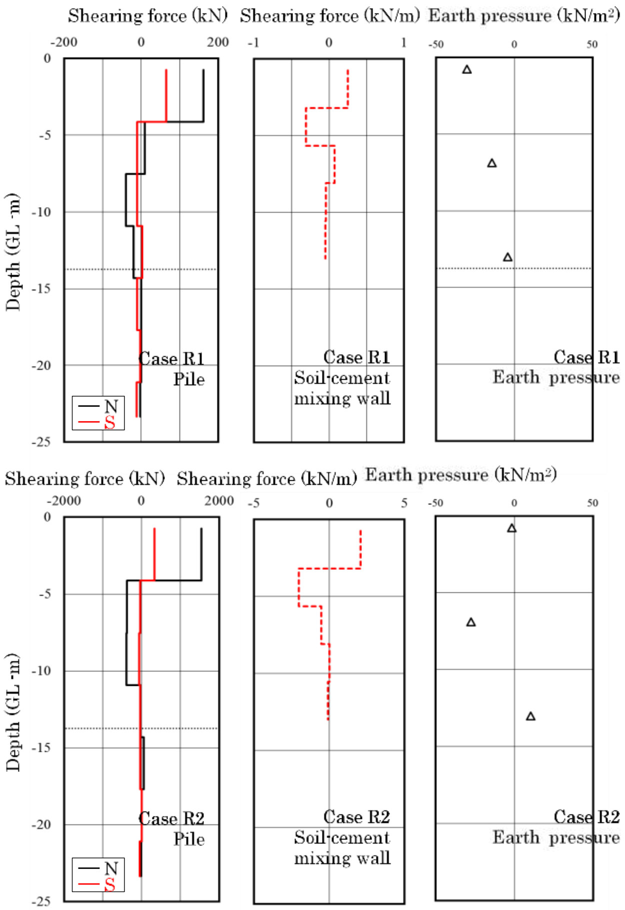

Figure 9. Distribution of shear force and earth pressure (Case R1 and R2)

dotted lines in the figure show the bending strain values at the time of test specimen fracture when the four-point bending tests were conducted on the pile model. As observed in Figure 10, although almost no residual strain was generated on the Model S pile, a considerable residual strain was generated on the Model N pile. In particular, for the excitation with maximum input acceleration of 4.4 m/s^2, the bending strain on Model N at GL-3.0 m reached a value that was the same as the strain measured at the time of fracture in the bending test, and it is concluded that the bending fracture of the pile occurred at this time. For the excitation with maximum input acceleration of 6.0 m/s^2, the bending strain on Model N at GL-0.75 m reached a value that was the same as the strain measured at the time of fracture in the bending test, and it is concluded that the bending fracture near the pile head of Model N occurred at this time. Photo 1 shows the model structure after all the excitation tests were completed. As explained previously, Photo 1 shows the bending fracture of the Model N pile near the pile head and at GL-3 m. In contrast, the Model S pile had no damage, demonstrating that the soil–cement mixing wall contributed to the reduction in the stress acting on the pile even under extreme conditions.

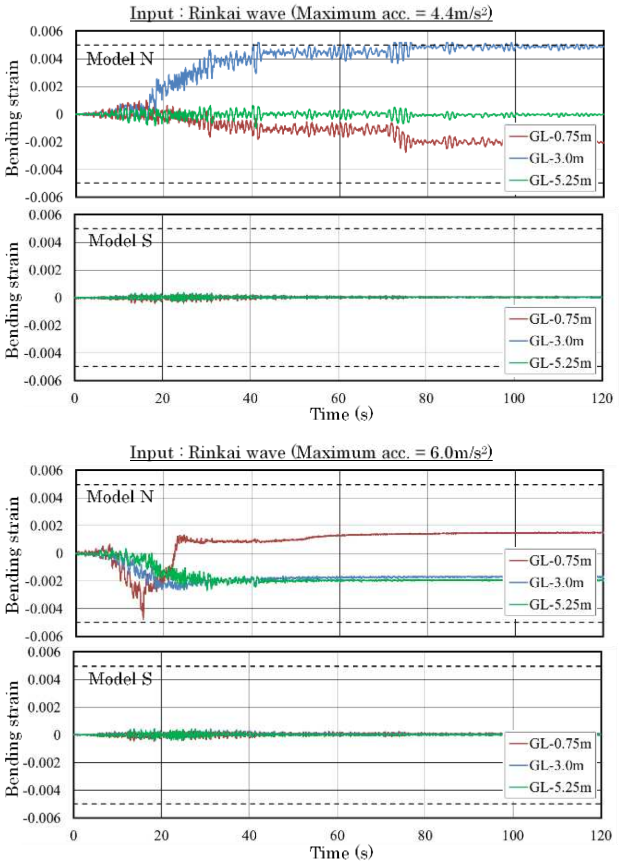

Figure 10. Time history curves of bending strain of pile during large input waves

Photo 1. Structure model after large shaking

4 RESULTS OF CENTRIFUGE SHAKING TABLE TESTS

The following observations were made from the centrifugal shaking table tests of the foundation structures wherein the soil–cement mixing wall was used as a permanent pile:

1) Depending on the excitation characteristics of the input wave, using the soil–cement mixing wall as a permanent pile may result in amplifying the structure's response.

2) It has been confirmed that using the soil–cement mixing wall as a permanent pile can reduce the maximum bending moment and the maximum shearing force generated on the pile.

3) In order to evaluate the reduction effect of the stress distribution and the stress generated on the pile, it is necessary to appropriately evaluate the effect of the earth pressure and the friction acting on the soil–cement mixing wall. In particular, the in-plane friction on the wall plays a dominant role in the reduction of the shearing force generated on the pile.

5 REFERENCES

Kaneko, O. 2004. Load-Displacement Relationships on Soil-cement H-shaped Pile, *Proceedings of 49th Geotechnical Symposium*: 127-132 (In Japanese).

Kaneko, O. and Isemoto, A. 2004. Seismic Behavior on Structure Surrounding Soil-cement Mixing Wall in Hyogo-ken Nanbu Earthquake, *Proceedings of 10th Japan Earthquake Engineering Symposium*: 401-406 (In Japanese).

Taya, Y. et al. 2009. A Study on Soil-cement Mixing Wall Using Permanent Pile (Part1 and 2), *Proceedings of Japan National Conference on Architecture*, Structure 1: 667-670 (In Japanese).

Watanabe, K. et al. 2013. In-situ Full Scale Load Test of Soil-cement Mixing Wall, *Proceedings of Japan National Conference on Architecture*, Structure 1: 487-488 (In Japanese).

Watanabe, K. et al. 2014. A Study on Bonding Behavior on Soil-cement Mixing Wall Using Permanent Pile, *Proceedings of Japan National Conference on Architecture*, Structure 1: 437-438 (In Japanese).

Watanabe, K. et al. 2015. In-situ Full Scale Load Test of Soil-cement Mixing Wall Using Permanent Pile, *Proceedings of Japan National Conference on Architecture*, Structure 1: 451-452 (In Japanese).